Acta Pharmacologica Sinica (2013) 34: 441–452
 1671-4083/13 $32.00
www.nature.com/aps

Original Article

Design, synthesis and biological evaluation of bivalent ligands against A_1–D_1 receptor heteromers

Jian SHEN, Lei ZHANG, Wan-ling SONG, Tao MENG, Xin WANG, Lin CHEN, Lin-yin FENG*, Ye-chun XU*, Jing-kang SHEN*

The State Key Laboratory of Drug Research, Shanghai Institute of Materia Medica, Chinese Academy of Sciences, Shanghai 201203, China

Aim: To design and synthesize bivalent ligands for adenosine A_1–dopamine D_1 receptor heteromers (A_1–D_1R), and evaluate their pharmacological activities.
Methods: Bivalent ligands and their corresponding A_1R monovalent ligands were designed and synthesized. The affinities of the bivalent ligands for A_1R and D_1R in rat brain membrane preparation were examined using radiolabeled binding assays. To demonstrate the formation of A_1–D_1R, fluorescence resonance energy transfer (FRET) was conducted in HEK293 cells transfected with D_1-CFP and A_1-YFP. Molecular modeling was used to analyze the possible mode of protein-protein and protein-ligand interactions.
Results: Two bivalent ligands for A_1R and D_1R (20a, 20b), as well as the corresponding A_1R monovalent ligands (21a, 21b) were synthesized. In radiolabeled binding assays, the bivalent ligands showed affinities for A_1R 10–100 times higher than those of the corresponding monovalent ligands. In FRET experiments, the bivalent ligands significantly increased the heterodimerization of A_1R and D_1R compared with the corresponding monovalent ligands. A heterodimer model with the interface of helixes 3, 4, 5 of A_1R and helixes 1, 6, 7 from D_1R was established with molecular modeling. The distance between the two ligand binding sites in the heterodimer model was approximately 48.4 Å, which was shorter than the length of the bivalent ligands.
Conclusion: This study demonstrates the existence of A_1–D_1R *in situ* and a simultaneous interaction of bivalent ligands with both the receptors.

Keywords: G protein-coupled receptors; adenosine; dopamine; A_1 receptor; D_1 receptor; heterodimers; bivalent ligands; radiolabeled binding assay; FRET; molecular modeling

Acta Pharmacologica Sinica (2013) 34: 441–452; doi: 10.1038/aps.2012.151; published online 21 Jan 2013

Introduction

G protein-coupled receptors (GPCRs) constitute the largest protein family of cell surface receptors, and they mediate a variety of signaling processes. Over the last 30 years, many researchers have identified that GPCRs can form dimeric and higher-order oligomers in natural tissues[1, 2]. In comparison with the constituting receptors, GPCR heteromers, which have different characteristics, are important for the understanding of receptor function and pharmacology. As a result, bivalent ligands are currently being developed as a promising strategy for drug discovery[3, 4].

The adenosine A_1 and dopamine D_1 receptors belong to the superfamily of GPCRs. Evidence for the existence of A_1R and D_1R heteromers has been presented and is based on immunoprecipitation and double immunolabeling experiments[5]. There are two subtypes of striatal GABAergic efferent neurons, projecting to the thalamus across two distinct pathways: the striato pallidal neurons (indirect pathway) and the striatonigrostriatoentopeduncular neurons (direct pathway). Evidence indicates that A_1R and D_1R are coexpressed in the basal ganglia and prefrontal cortex, which are particularly involved in the direct pathway[6]. In rat models of Parkinson's disease, the motor activating effects of the D_1 agonist, SKF38393, were enhanced by the A_1 receptor antagonist[7]. This synergistic mechanism may provide some insight into the design of novel agents for the treatment of Parkinson's disease and neuropsychiatric disorders based on the pharmacological properties of the A_1–D_1 heteromeric complex[5].

Although heteromerization was reported in native tissues, there is no direct evidence to prove the existence of A_1–D_1 receptor heterodimerization. A_1–D_1 bivalent ligands could be important research tools to detect heterodimerization and further explore the biological functions of A_1–D_1 receptor het-

* To whom correspondence should be addressed.
E-mail: jkshen@mail.shcnc.ac.cn (Jing-kang SHEN);
lyfeng@mail.shcnc.ac.cn (Lin-ying FENG);
ycxu@mail.shcnc.ac.cn (Ye-chun XU)
Received 2012-05-31 Accepted 2012-10-08

erodimers.

Bivalent ligands are molecules that consist of two pharmacophores linked by a spacer[8]. Recently, synthesis and biological investigations of bivalent ligands were described to target serotonin[9], muscarinic[10], opioid[11] and other receptors. Rafael Franco and Miriam Royo designed bivalent ligands targeting $A_{2A}R$–D_2R heterodimerization, which contained a D_2R agonist, a $A_{2A}R$ antagonist and their corresponding monovalent control compounds. Their results indicated that the existence of $A_{2A}R$–D_2R heterodimerization and a simultaneous interaction of bivalent ligands with both receptors[12].

We designed and synthesized a group of bivalent ligands containing a D_1R agonist and a A_1R antagonist linked by different lengths of PEG linkers. The binding properties of these compounds were determined by radioligand binding studies in membrane preparations from brain striatum. FRET experiments were performed to test if these bivalent ligands can promote the formation of A_1R and D_1R heterodimers (Figure 1).

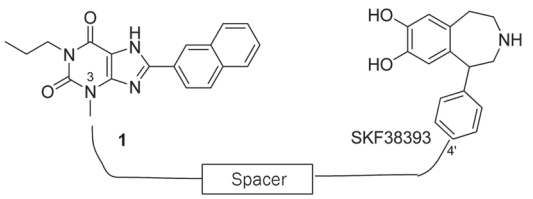

Figure 1. General structure of bivalent ligands.

Materials and methods

Chemistry

Compound design

A_1–D_1 bivalent ligands were designed by combining two pharmacophoric entities with different lengths of linkers. First, compound **1**, a naphthylxanthine derivative, was chosen as the A_1 antagonist pharmacophore. Then, SKF38393, a 1-aryl-3-benzazepine analog that displays high binding affinity at the D_1 receptor, was selected as the D_1 agonist pharmacophore. Structure-activity relationship indicated that the N-3 site of compound **1** and 4′ site of SKF38393 are not active sites[13–16]. Thus, linkers were introduced at these sites to combine the A_1 antagonist and D_1 agonist pharmacophores.

Polyethylene glycol (PEG) is widely used due to its low toxicity, excellent aqueous solubility and low antigenicity. Recently, Kiessling *et al* found that an unexpected enhancement in the biological activity of a GPCR ligand was induced by a polyethylene glycol substitute[17]. Considering the fact that PEG has a moderate ΔS_{tor} (the entropy associated with torsional motions about a single bond)[18], PEG was chosen as the linker for the selected pharmacophores. Recently, Gmeiner *et al* reported the synthesis and biological investigation of bivalent ligands for D_2-like receptors. Bivalent ligands, linked by 5–8 oligoethylene glycol units, showed up to a 70-fold increase of D_3 binding affinity compared to monovalent ligand compounds[19]. As a result, we designed bivalent ligands linked by 4 and 6 oligoethylene glycol units.

We also synthesized the corresponding monovalent ligand compounds for the A_1 antagonist as a control to determine whether the bivalent ligands showed improved affinity for the A_1 receptor compared to the monovalent ligand controls. In 1991, Neumeyer *et al* synthesized the derivative of SKF38393 to identify effective fluorescent probes. However, coupling of the large group to the 4′ site of SKF38393 resulted in a considerable loss of affinity[20]. As a result, we did not synthesize the corresponding monovalent ligand compounds for the D_1 antagonist as a control.

Preparation of the bivalent ligands and their monovalent ligands

Bivalent ligands linked by PEG chains were synthesized by the route demonstrated in Scheme 1. Commercially available polyethylene glycol was easily converted to compound **2a–2b** using acrylonitrile via the Michael addition reaction. Reduction of compound **2a–2b** with borane produced the compound **3a–3b**.

The synthesis of the common intermediate, compound **4,** has previously been described[13]. Treatment of compound **4** with ethyl 4-bromobutanoate produced compound **5**. Then, compound **5** was heated in 20% NaOH (aq), followed by ring closure, to generate compound **6**. Compound **6** was coupled with **3a–3b** in the presence of PyBop/DIPEA in DMF to yield **7a–7b**.

Commercially available nitroacetophenone was transformed into compound **8** using a catalytic amount of Lewis acid. The reaction of **8** with $NaBH_4$ produced compound **9**. Compound **9** and commercially available 3,4-dimethoxy phenylethylamine were heated at reflux in THF to yield compound **10**. Compound **10** was heated in PPA, followed by ring closure, to produce the cyclization compound **11**. The reaction of **11** with iron powder generated compound **12**. The addition of a Nosyl group to **12** in the presence of basic conditions yielded compound **13**. Compound **13** was converted to **14** via a Mitsunobu reaction. Deprotection of compound **14** with BBr_3 at -78 °C produced compound **15** without future purification. The addition of a MOM group to **15** under basic conditions produced compound **16**. Compound **17** was easily obtained from **16** via an ester hydrolysis reaction.

Compounds **18a–18b** were obtained from **17** and **7a–7b** using standard peptide synthesis procedures, with EDCI/HOBt as the catalytic coupling agents. Removal of the Nosyl group in **18a–18b,** in the presence of K_2CO_3 and PhSH, yielded compound **19a–19b**. Deprotection of compound **19a–19b** with BBr_3 at -78 °C gave the target compound **20a–20b** (Scheme 1).

Monovalent ligands were synthesized, and the route is demonstrated in Scheme 2. Compounds **21a–21b** were obtained using hexanoic acid, and **7a–7b** were obtained using standard peptide synthesis procedures, with EDCI/HOBt as the catalytic coupling agents.

Reagents and conditions

a) acrylonitrile, THF, 60 °C, 1.5 h (99%); b) BH_3, THF, 60 °C, 3.5 h (97%); c) ethyl 4-bromobutanoate, DBU, DMF, 60 °C, 48 h

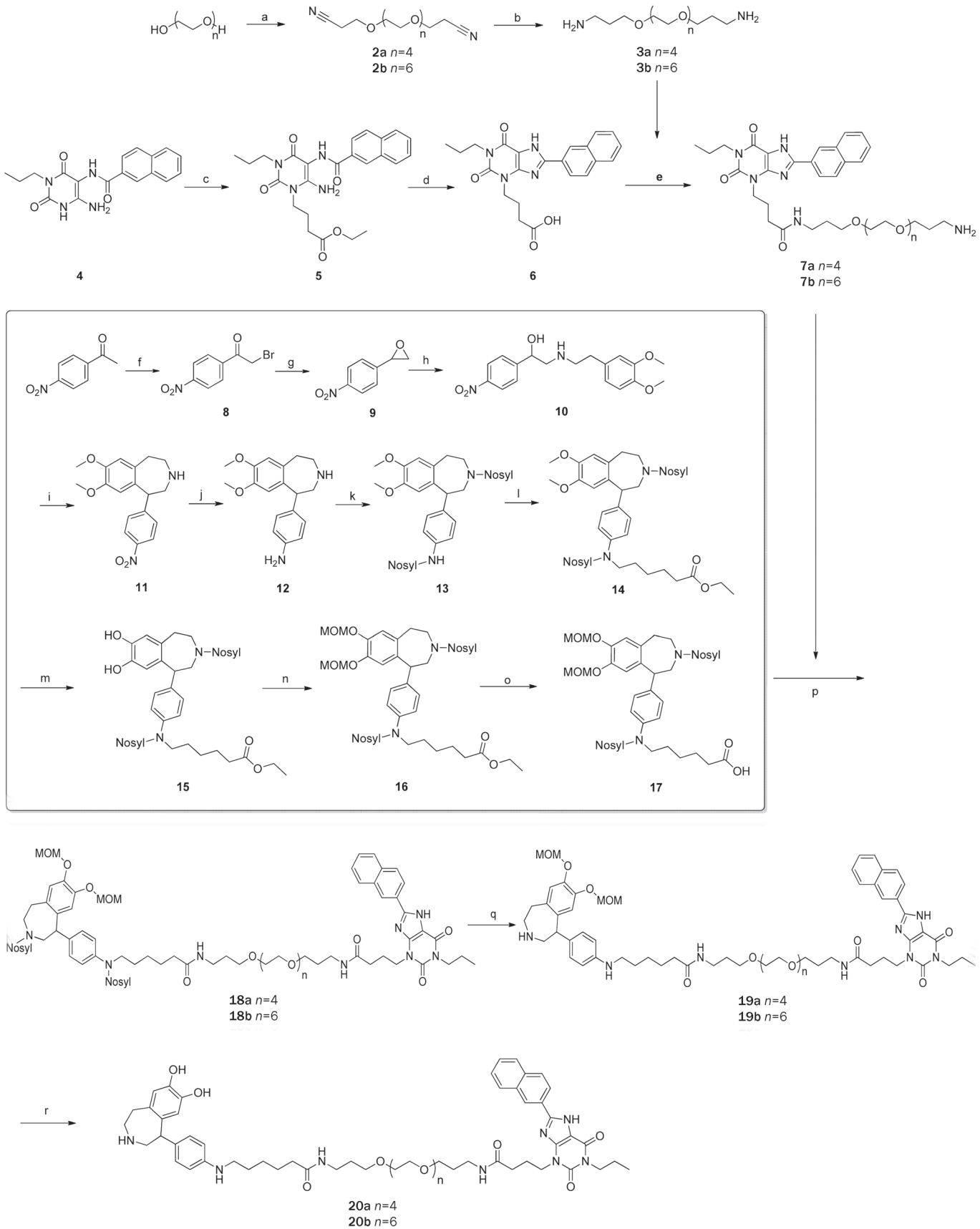

Scheme 1. Synthesis of the bivalent ligands linked by PEG.

(44%); d) 20% NaOH (aq), 60 °C, 3 h (61%); e) PyBOP, DIPEA, DMF, rt, overnight (60%); f) Br_2, $AlCl_3$ (Cat.), Et_2O, 0 °C, rt, 3 h (95%); g) $NaBH_4$, 2 mol/L NaOH (aq), THF-MeOH, 0 °C, rt, 35 min (69%); h) 3,4-dimethoxyphenylethylamine, THF, reflux overnight (56%); i) PPA 100 °C, 1 h (75%); j) Fe powder, HCl (aq), EtOH-H_2O, reflux for 1 h (40%); k) Nosyl-Cl, Et_3N, DCM, 0 °C, rt, overnight (80%); l) Ph_3P, DIAD, hex-4-yn-1-ol, rt, overnight (80%); m) BBr_3,CH_2Cl_2, -78 °C, rt, overnight; n) Bromomethyl methyl ether, DIPEA, rt, overnight; o) 2 mol/L NaOH(aq), THF, CH_3OH, rt, 1 h (70%); p) EDCI, HOBt, DIPEA, DMF, rt, overnight (40%); q) PhSH, K_2CO_3, 80 °C, overnight (60%); r) TFA, DCM, rt, 1 h (60%).

Receptor binding assay

A P2 membrane fraction was prepared from whole brains of adult Wistar rats (200–300 g). The tissue was homogenized in 10× (*w/v*) 10% sucrose solution, and the suspension was centrifuged at 1000×*g* for 10 min (4 °C). The supernatant was decanted and retained on ice. The pellet was resuspended in 50 mmol/L Tris-HCl buffer (pH=7.4) at 1:5 (*w/v*). Then, the Lowry method was employed to determine the protein concentration. All the solutions were diluted to 2 mg/mL and stored at -80 °C.

In the D_1 receptor competitive assay, compound samples, the D_1 receptor antagonist, [^{3}H]-SCH23390 (0.5 nmol/L) and 200 μg of rat cortex membrane protein mixture were added to each tube. All of the above operations were performed in an ice bath. The sequence in which the samples were added and their volumes are listed in Table 1. The final volume was adjusted to 200 μL with Tris-HCl buffer (Tris-HCl 50 mmol/L, NaCl 120 mmol/L, KCl 5 mmol/L, $MgCl_2$ 1 mmol/L, $CaCl_2$ 2 mmol/L, pH 7.4). The tubes were kept in a 37 °C water bath for 30 min. Twenty microliters of Tris-HCl buffer was used to replace the sample in the total binding tube, and 20 μL of SCH23390 (0.1 mg/mL) was used to replace the sample in the nonspecific binding tube.

Table 1. The protocol of competitive binding assay.

	Serial number	[^{3}H]Ligand (μL)	Ligand (μL)	Drug (μL)	Tris-HCl (μL)	Protein (μL)
Total binding	1, 2, 3	20	–	–	20	160
Nonspecific binding	4, 5, 6	20	20	–	–	160
Sample	7, 8, 9	20	-	20	–	160
...	...	20	-	20	–	160

In the A_1 receptor competitive binding assay, compounds of the A_1 receptor antagonist, [^{3}H]-DPCPX, and 200 g rat cortex membrane protein mixture were added to each tube. The final volume was adjusted to 200 μL with Tris-HCl buffer (Tris-HCl 50 mmol/L, NaCl 120 mmol/L, KCl 5 mmol/L, $MgCl_2$ 1 mmol/L, $CaCl_2$ 2 mmol/L, pH 7.4). The tubes were kept in a 37 °C water bath for 30 min. Twenty microliters of Tris-HCl buffer was used to replace the sample in the total binding tube, and 20 μL of the specific ligand, DPCPX (10 μmol/L) was used to replace the sample in the nonspecific binding tube.

When the water bath was finished, the reaction buffer was immediately filtered using a Brandel 24-well cell collector and GF/B filter to stop the reaction. The filter was washed three times with ice-cold 50 mmol/L Tris-HCl buffer (pH=7.4). After the filter was dry and transferred to a 0.5 mL EP, flashing liquid was added and a MicroBeta2 porous plate was used to measure the radiation activity. The equation for calculating the inhibition rate was as follows:

$$\text{Inhibition rate (\%)} = 100 - (cpm_{sample} - cpm_{non\text{-}specific\ binding}) / (cpm_{total\ binding} - cpm_{non\text{-}specific\ binding}) \times 100$$

Non-linear regression implemented using GraphPad Prism 4.0 (GraphPad Software Inc) was used to calculate the IC_{50}.

Measurement of FRET efficiency in HEK293 cells

FRET technology detects protein-protein interactions in live cells with high sensitivity[21]. FRET occurs when a donor chromophore, initially in its electronic excited state, transfers energy to a nearby acceptor chromophore (10–100 Å) through non-radiative dipole-dipole coupling. The adenosine A_1 receptor and dopaminergic D_1 receptor form heterodimers when co-localized. This experiment employs FRET technology to screen for compounds that promote the formation of A_1R and D_1R heterodimers.

HEK293 cells were transiently transfected with plasmid DNA corresponding to the D_1-CFP (acceptor) and A_1-YFP (donor), with a ratio of donor to acceptor DNA of 1:1. GFP-YFP plasmids were used as a control. A mixture of cells separately transfected with either A_1 YFP or D_1 CFP (A_1YFP+D_1CFP) were used as negative controls. HEK293 cells were transfected with the plasmids using the Trans Messenger Transfection Reagent (QIAGEN) for 48 h before collection with cold D-Hanks' buffer. The cells were washed twice, resuspended and seeded into 96-well plates at a density of 1×10^5 cells/well for fluorescence detection. Fluorescence intensity

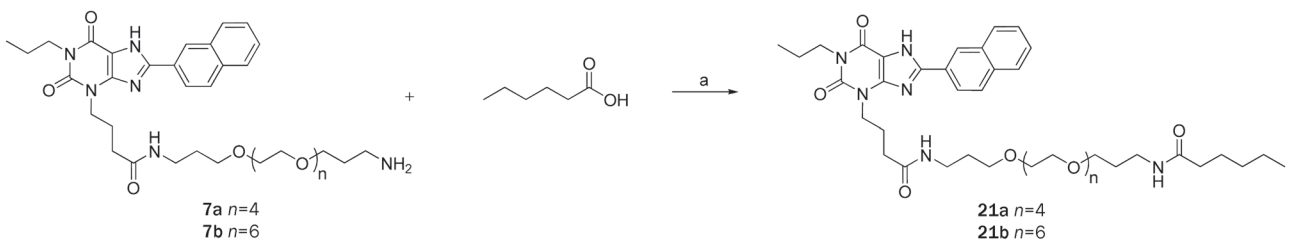

7a *n*=4
7b *n*=6

21a *n*=4
21b *n*=6

Scheme 2. Synthesis of the monovalent ligand compounds. Reagents and conditions: a) EDCI, HOBt, DIPEA, DMF, rt, overnight (70%).

was measured with a double-channel Novo star fluorescent spectrophotometer (channel1: excitation wavelength 440 nm, emission wavelength 520 nm; channel 2: excitation wavelength 440 nm, emission wavelength 470 nm). The energy transfer efficiency (FRET efficiency) was calculated using the following formula:

$$\text{FRET efficiency}=F_{440/520}/F_{440/470}.$$

$F_{440/520}$ was the fluorescence intensity detected through channel 1, and $F_{440/470}$ was the fluorescence intensity detected through channel 2. The excitation wavelength for CFP was 440 nm and for YFP was 520 nm, and 470 nm was the emission wavelength for CFP.

Ligand docking studies

Homology models of the adenosine A_1 receptor and dopamine D_1 receptor were built using Modeller 9.10. The model of the A_1 receptor was constructed using the crystal structure of the adenosine A_{2A} receptor (PDB code: 3EML) as a template[22]. The model of the D_1 receptor was constructed using multiple templates from the crystal structures of Rhodopsin (PDB code: 1U19)[23], the β_2 adrenergic receptor (PDB code: 2RH1)[24], the histamine H_1 receptor (PDB code: 3RZE)[25], the S1P1 receptor (PDB code: 3V2Y)[26], and the dopamine D_3 receptor (PDB code: 3PBL)[27]. All the alignments were generated using Modeller 9.10, using default settings that were manually modified afterwards with careful attention to the alignment of all the conserved residues. The 'Biopolymer structure preparation' protocol of Sybyl 7.5 was used to prepare the models, and the minimization tool of Sybyl 7.5 was used to minimize all the models stepwise from hydrogen side-chains and main-chains to whole molecule minimization. The dopamine D_1 receptor models were later subjected to molecular dynamics (MD) simulation using Gromacs 4.5 for further refinement of the long ECL2. The MD simulation was performed for 40 ns using the CHARMM27 force field, and all the heavy atoms, except those on ECL2, were restrained by a constant force of 100 000 ($kJ\cdot mol^{-1}\cdot nm^{-2}$). The production runs were conducted using NTP ensemble at 300K, with a 1 fs time-step integration. The Particle Mesh Ewald method (PME) was used to calculate the electrostatic contribution to non-bonded interactions, with a cutoff of 9 Å and a time step of 1 fs. The cutoff distance of the van der Waals interaction and coulomb interaction were 14 Å and 9 Å, respectively. The LINCS algorithm was applied to the system. All the models were evaluated and validated using PROCHECK and the Pro-SA web server.

Autodock 4.2 was used to search for the binding conformation of compound **1** and SKF38393 in the A_1 receptor and D_1 receptor, respectively. A binding box of 19×19×22 Å, centered at the binding cavity, was used, and 100 conformations were generated for each ligand using genetic algorithm. The binding conformation was chosen from the largest cluster (cluster tolerance was determined using default settings) and validated with the available mutation experiment data.

The ZDOCK protocol in Discovery studio 2.5 suite was used to search the heterodimer interface. Default parameters were used, and the results were selected manually. The PEG linker was added to the heterodimer and minimized using Sybyl 7.5.

Results

Chemistry

The bivalent ligands, **20a–20b,** and monovalent ligands, **21a–21b,** were designed and synthesized through the route outlined in Scheme 1. All the compounds were purified by silica gel thin-layer chromatography (>95%), and their structures were determined by nuclear magnetic resonance spectra and low-resolution mass spectra. Details of their structures are shown in Table 2.

Receptor binding assay

The binding affinity assay was performed using the bivalent ligands, **20a–20b,** with 4 and 6 polyethylene glycol units, respectively, along with their monovalent ligands, **21a–21b**. As expected, the bivalent ligands, **20a–20b,** showed moderate binding for the A_1 receptor and D_1 receptor, while the monovalent control ligands, **21a–21b,** showed moderate binding for the A_1 receptor. However, there was no correlation between linker length and binding affinity for the bivalent ligands, **20a–20b**. It is possible that the high flexibility of the PEG linker could explain this phenomenon. The affinities for A_1R was 10–100 times higher for bivalent ligands compared with their monovalent controls. These results are summarized in Table 2.

Measurement of FRET efficiency in HEK293 cells

FRET technology detects protein-protein interactions in live cells with high sensitivity. The adenosine A_1 receptor and dopaminergic D_1 receptor form heterodimers when co-localized. This experiment employed FRET technology to screen for compounds that promote the formation of A_1R and D_1R heterodimers.

As shown in Figure 2, A_1YFP+D_1CFP represents the cells transfected with either A_1YFP or D_1CFP, set as the negative control. CFPYFP represents the positive control. A_1YFP/D_1CFP indicates the cells co-transfected with both D_1-CFP and

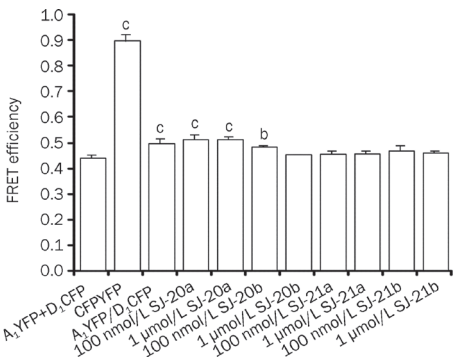

Figure 2. Fluorescence resonance energy transfer (FRET) experiment confirmed bivalent ligands promoting the formation of heterodimers of A_1R and D_1R. $^bP<0.05$, $^cP<0.01$ *vs* negative control group.

Table 2. Binding affinity of bivalent and monovalent ligands to A_1R and D_1R in brain striatum membranes.

Name	Structure	A_1 IC_{50} (μmol/L)	D_1 IC_{50} (μmol/L)
1	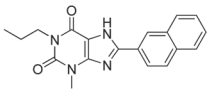	0.092	NA
SKF38393	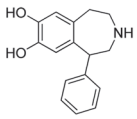	NA	0.47
20a	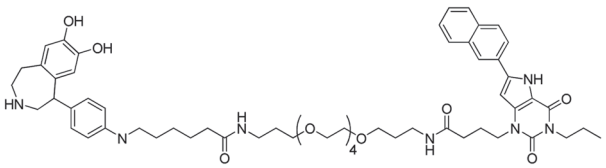	0.29	3.13
20b	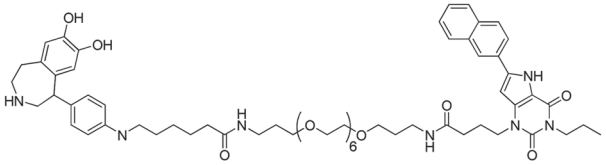	0.44	1.98
21a	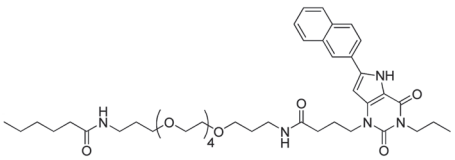	3.65	NA
21b	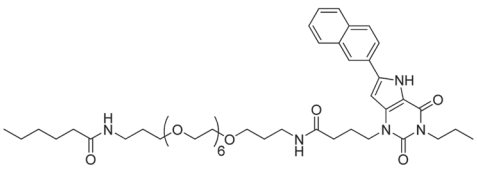	48.87	NA

A_1-YFP. Plates were read 48 h after the transfection was finished. Parameters of the spectrophotometer were set according to the manual.

FRET efficiency values were obtained from the positive control, in which the cells co-transfected with A_1YFP/D_1CFP differed significantly compared to the negative control group (cells transfected with either A_1YFP or D_1CFP, $P<0.01$). Similar significant differences in the FRET efficiency values were also detected in cells treated with 100 nmol/L **20a**, 1 μmol/L **20a** or 100 nmol/L **20b** compared to the negative control cells. These results indicate that the bivalent ligands, **20a–20b,** increased the heterodimerization of the A_1 receptor and D_1 receptor to a higher extent than the monovalent control ligands, **21a–21b**. It was consistent with that of the receptor binding assay.

Ligand docking studies

A docking experiment was performed to confirm the length of the linker and the bivalent ligand binding mode. The A_1–D_1 heterodimer interface was searched by ZDOCK and checked manually based on the ZDOCK score and associated bioinformatics data. Tarakanov and Fuxe deduced a set of triplets that may be responsible for receptor-receptor interactions[28, 29]. Leucine-rich motifs, one type of these triplets, are charged residues that may serve as an 'adhesive guide' for the formation of strong bonds between the amino acids of two receptors. As seen in Figure 3, the homology triplets, ILS and AAV, exist in helix 4 of A_1 and helix 1 of D_1. Combined with the docking rank, we established a heterodimer model with the interface of helixes 3, 4, and 5 of the A_1 receptor and helixes 1, 6, and 7 from the D_1 receptor (Figure 4). The distance between the two ligand binding sites in this heterodimer model is approximately 48.4 Å, which is shorter than the length of the bivalent ligands. The linker of **20b** was manually added to the docked ligands in the heterodimer model and minimized with Sybyl tools. As shown in Figure 4, the linker tightly interacts with ECL2 and ECL1 of the A_1 receptor and D_1 receptor. Moreover,

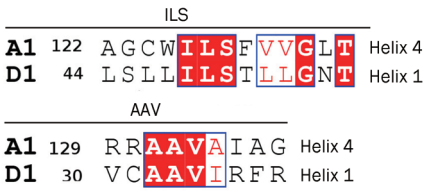

Figure 3. Analysis of sequence and alignment of A_1 receptor and D_1 receptor in silico receptor.

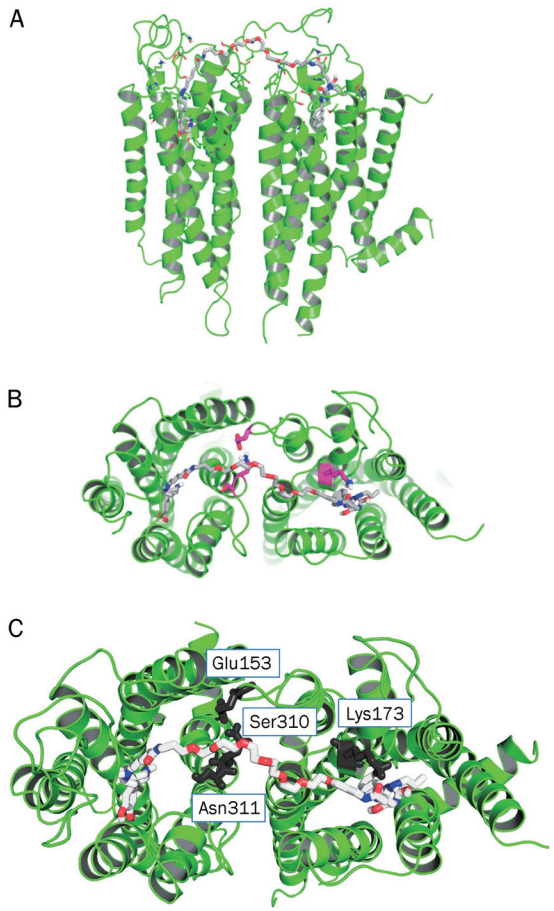

Figure 4. Energy minimized heterodimer model with compound **20b** binding. The left is D_1 receptor and the right A_1 receptor. (A) The side view of the compound **20b** binding in the heterodimer. Ligand colored grey and the residues interacting with it are shown in lines. (B) The top view of the compound **20b** binding in the heterodimer. Residues that form hydrogen bonds with PEG linker are shown in sticks and colored magentas. (C) Bivalent ligand is shown in sticks and colored white. Residues that form hydrogen bonds with PEG linker are shown in sticks and colored black. These residues include: Glu153, Lys173 from A_1 receptor and Asn311, Ser310 from D_1 receptor.

the oxygen atoms on the PEG linker form polar interactions with the polar residues on the extracellular loops of the heterodimer, which enhances the binding ability of the bivalent ligand to the heterodimer. The ligand docking studies verify that the bivalent ligand binds to both binding sites in the heterodimer.

Discussion

According to the binding assay results shown in Table 2, bivalent ligands **20a–20b** showed moderate binding for the A_1 and D_1 receptors, while monovalent control ligands **21a–21b** only showed moderate binding for the A_1 receptor. The affinity for A_1R was 10–100 times higher for bivalent ligands compared with their monovalent controls. One possible reason for this phenomenon is conformational crosstalk within one receptor protomer or modulation of the interaction between two protomers of a receptor dimer induced by positive cooperativity. Positive cooperativity can also be induced when bivalent ligands bind two adjacent binding sites of A_1–D_1 receptor heteromers because binding of the second pharmacophore is significantly accelerated due to the vicinity of ligand, thus facilitating local concentration enrichment. As a result, a bivalent ligand that binds to D_1R may subsequently have a higher affinity with A_1R located in the near vicinity compared to the corresponding A_1R monovalent ligand[9, 30]. These data indicate the specific interaction of these bivalent ligands with A_1–D_1 receptor heteromers and suggest that these ligands could be useful as pharmacological tools to detect receptor heteromers in native tissue.

FRET technology has been decisive for demonstrating heteromer formation in heterologous expression systems. This study employed FRET technology to screen for bivalent ligands that promote the formation of A_1R and D_1R heterodimers. FRET efficiency values obtained from cells co-transfected with A_1YFP/D_1CFP differed significantly compared to those of the negative control group. Similar significant differences were also observed in the FRET efficiency values of cells treated with bivalent ligands compared to the negative control cells. These results confirm that bivalent ligands can detect the presence of heterodimers of A_1R and D_1R.

The docking experiments showed that the linker of the bivalent ligands is long enough to allow for the two pharmacophoric moieties to bind an A_1–D_1 heterodimer. The minimum distance between the two ligand binding sites in this heterodimer model was 48.4 Å. This length is similar to the one proposed for other GPCR dimers, such as A_{2A}–D_2 receptor heterodimers. As shown in Figure 4, the linker has a tight interaction with ECL2 and ECL1 of the A_1 and D_1 receptors. Moreover, the oxygen atoms on the PEG linker form polar interactions with the polar residues on the extracellular loops of the heterodimer, which enhances the binding ability of the bivalent ligand to the heterodimer. Ligand docking studies verify that bivalent ligands bind to both binding sites in the heterodimer.

Conclusion

This report provides evidence for the existence of A_1R and D_1R heteromers. However, in native tissues, there is no direct evidence to prove the existence of A_1–D_1 receptor heterodimerization. In the present study, we designed and synthesized a

set of the bivalent ligands, differing in length, that link two different pharmacophores. The binding affinities for bivalent ligands for A_1R were 10–100 times higher compared with their monovalent controls. The results of the binding assays revealed the specific interaction of these bivalent ligands with A_1–D_1 receptor heteromers. FRET efficiency values obtained from cells co-transfected with 100 nmol/L **20a**, 1 μmol/L **20a** or 100 nmol/L **20b** differed significantly compared to those of the negative control group. These results confirmed that bivalent ligands can detect the presence of A_1R and D_1R heterodimers. The docking experiments also verified that bivalent ligands act on both binding sites of the heterodimer and indicated the possible length of the linker. In summary, we designed and synthesized bivalent ligands that act as molecular probes for A_1–D_1 receptor heteromers. A_1–D_1 bivalent ligands might be an important research tool to detect heterodimerization and explore further biological functions of A_1–D_1 receptor heterodimers. Further studies are in progress.

Appendix

The chemical reagents (chemicals) were purchased from Lancaster, Acros, and Shanghai Chemical Reagent Company which were used without further purification. ^{1}H- and ^{13}C-NMR spectra were recorded in DMSO-d_6 or $CDCl_3$ on Varian Mercury-300 or Varian Mercury-400 instruments. The ESI-MS were carried out on Thermo Finnigan LCQDECAXP. TLC was carried out with glass pre-coated silica gel GF254 plates.

4,7,10,13,16-pentaoxanonadecane-1,19-dinitrile (2a)

In a RB flask, was added acrylonitrile (50 mL, 0.76 mol), 2,2′-(2,2′-oxybis(ethane-2,1-diyl)*bis*(oxy))diethanol (6.53 g, 33.67 mmol) and KOH (28.8 mg, 0.51 mmol), the reaction mixture was stirred at rt for 1.5 h. The reaction was quenched with several drops of HCl (6 mol/L), the solvent was evaporated under vacuo, the residue was dissolved in DCM, filter through celite, the filtrate was evaporated to dryness to give the title compound as yellow oil without further purification (7.75 g, 99%); LRMS (ESI) *m/z* 301 $[M+H]^+$.

4,7,10,13,16,19,22-Heptaoxapentacosanedinitrile (2b)

Compound **2b** (yield 98 %) was prepared according to the method described for the preparation of compound **2a**; LRMS (ESI) *m/z* 389 $[M+H]^+$.

4,7,10,13,16-pentaoxanonadecane-1,19-diamine (3a)

To a solution of compound **3a** (4 g, 13.3 mmol) in dry THF (30 mL) stirred under N_2 at 0 °C, was added 1 mol/L BH_3-THF (100 mL, 100 mmol) dropwise during 30 min. The reaction mixture was heated to reflux for 3.5 h. Then the reaction was quenched with MeOH (30 mL) and HCl (7 mL) at 0 °C. After removing of the solvent, the residue was dissolved in 2 mol/L NaOH (50 mL), extracted with DCM (25 mL*15), dried over Na_2SO_4, filtered and concentrated to give the title compound as colorless oil without further purification (4.01 g, 97%); LRMS (ESI) *m/z* 309 $[M+H]^+$.

4,7,10,13,16,19,22-heptaoxapentacosane-1,25-diamine (3b)

Compound **3b** (yield 98%) was prepared according to the method described for the preparation of compound **3a**; LRMS (ESI) *m/z* 397 $[M+H]^+$.

N-(6-amino-1-(3-hydroxypropyl)-2,4-dioxo-3-propyl-1,2,3,4-tetrahydropyrimidin-5-yl)-2-naphthamide (5)

To a solution of Compound **4** (1.2 g, 3.55 mmol) in dry DMF (50 mL) stirred under N_2 at rt, were added ethyl 4-bromobutanoate (2.03 mL, 14.2 mmol), DBU (0.72 mL, 7.1 mmol). The reaction mixture was stirred at 60 °C for 48 h. After cooling reaction, the solvent was removed under vacuo, the residue was dissolved in EtOAc (50 mL), washed with water and brine, dried over Na_2SO_4, filtered and concentrated. The crude product was purified by chromatography (2:1 petroleum ether-EtOAc) to give the title compound as an oil (700 mg, 44%); ^{1}H-NMR (300 MHz, DMSO-d_6): δ 9.08 (s, 1H), 8.62 (s, 1H), 8.07–7.98 (m, 4H), 7.63–7.60 (m, 2H), 6.79 (s, 2H), 4.10–4.05 (m, 2H), 3.92 (t, *J*=5.7 Hz, 2H), 3.73 (t, *J*=5.1 Hz, 2H), 2.38 (t, *J*=5.7 Hz, 2H), 1.84–1.80 (m, 2H), 1.55–1.49 (m, 2H), 1.19 (t, *J*=5.7 Hz, 3H), 0.84 (t, *J*=5.7 Hz, 3H).

3-(3-hydroxypropyl)-8-(naphthalen-2-yl)-1-propyl-1H-purine-2,6(3H,7H)-dione (6)

To a solution of Compound **5** (600 mg, 1.32 mmol) in methanol (120 mL) stirred at rt, was added 20% NaOH (11 mL). The reaction mixture was stirred at 60 °C for 3 h. After cooling the reaction, the solution was acidified by 2 mol/L HCl to adjust pH<3, the solid was collected by filter, dried to give the title compound as white solid (350 mg, 61%); ^{1}H-NMR (400 MHz, DMSO-d_6): δ 8.69 (s, 1H), 8.22 (d, *J*=8.8 Hz, 1H), 8.02–7.93 (m, 3H), 7.58–7.55 (m, 2H), 4.12 (t, *J*=6.4 Hz, 2H), 3.85 (t, *J*=7.2 Hz, 2H), 2.32–2.29 (t, *J=7.2*, 2H), 2.20–1.59 (m, 2H), 1.61–1.55 (m, 2H), 0.87 (t, *J*=7.6 Hz, 3H); LRMS (ESI) *m/z* 379 $[M+H]^+$; mp 190–194 °C.

N-(19-amino-4,7,10,13,16-pentaoxanonadecyl)-4-(8-(naphthalen-2-yl)-2,6-dioxo-1-propyl-1H-purin-3(2H,6H,7H)-yl)butanamide (7a)

To a solution of compound **6** (100 mg, 0.25 mmol) and **3a** (60 mg, 0.28 mmol) in dry DMF (10 mL) stirred at rt, were added PyBOP (143 mg, 0.28 mmol), DIPEA (88 μL, 0.5 mmol), the reaction mixture was stirred at rt overnight. The solvent was evaporated, the residue was purified by chromatography (10: 1 DCM-MeOH) to afford the title compound as a white solid (96 mg, 60%). ^{1}H-NMR (400 MHz, DMSO-d_6) δ 8.70 (s, 1H), 8.22–8.21 (m, 1H), 8.05-7.95 (m, 3H), 7.79 (m, 1H), 7.60–7.57 (m, 1H), 4.10 (t, *J*=8 Hz, 2H), 3.87 (t, *J*=9.1 Hz, 2H), 3.48–3.43 (m, 18H), 3.36–3.32 (m, 2H), 3.06–3.04 (m, 2H), 2.83 (t, *J*=9.6 Hz, 2H), 2.15 (m, 2H), 2.01–1.99 (m, 2H), 1.78–1.74 (m, 2H), 1.61–1.55 (m, 4H), 0.89 (t, *J*=9.6 Hz, 3H); LRMS (ESI) *m/z* 697 $[M+H]^+$.

N-(25-amino-4,7,10,13,16,19,22-heptaoxapentacosyl)-4-(8-(naphthalen-2-yl)-2,6-dioxo-1-propyl-1H-purin-3(2H,6H,7H)-yl) butanamide (7b)

Compound **7b** (yield 50%) was prepared according to the methodology described for the preparation of compound **7a.** ^{1}H-NMR (400 MHz, DMSO-d_6): δ 8.70 (s, 1H), 8.04–8.01 (m, 1H), 7.97–7.96 (m, 3H), 7.60–7.59 (m, 1H), 7.68–7.57 (m, 1H), 4.10 (t, *J*=8 Hz, 2H), 3.87 (t, *J*=9.1 Hz, 2H), 3.50–3.42 (m, 26 H), 3.34 (t, *J*=8.4 Hz, 2H), 3.06–3.04 (m, 2H), 2.82 (t, *J*=10.4 Hz, 2H), 2.16 (m, 2H), 2.03–1.96

(m, 2H), 1.78 (m, 2H), 1.61–1.55 (m, 4H), 0.89 (t, *J*=9.6 Hz, 3H); LRMS (ESI) *m/z* 785 $[M+H]^+$.

2-bromo-1-(4-nitrophenyl)ethanone (8)

To a solution of 4-nitroacetophenone (30 g, 0.18 mol) in dry ether (500 mL) stirred at 0 °C, was added $AlCl_3$ (cat), followed by Br_2 (10.3 mL, 0.20 mol). The reaction mixture was stirred at rt fot 3 h. Then the reaction was quenched with $Na_2S_2O_3$-$NaHCO_3$ (aq), extracted with DCM (400 mL*2), the combined organic phase was washed with brine, dried over Na_2SO_4, filtered and concentrated to give the title compound as yellow solid (42 g, 95%); ^{1}H-NMR (300 MHz, $CDCl_3$): δ 8.36–8.33 (m, 2H), 8.17–8.14 (m, 2H), 4.46 (s, 2H); LRMS (ESI) *m/z* 244 $[M+H]^+$; mp 76–79 °C.

2-(4-nitrophenyl)oxirane (9)

To a solution of compound **8** (43 g, 0.18 mol) in 150 mL CH_3OH-THF (V/V=1/1.2) stirred at 0 °C, was added $NaBH_4$ (6.8 g, 0.18 mol), followed by 2 mol/L NaOH (90 mL). The reaction mixture was stirred at rt for 35 min. The solvent was evaporated under vacuum, the residue was treated with HOAc to adjust pH=4, extracted with DCM (100 mL), the organic phase was washed with saturated $NaHCO_3$, water and brine, dried over Na_2SO_4, filtered and concentrated. The crude product was then purified by chromatography (10:1 petroleum ether-EtOAc) to give the title compound as yellow solid (20 g, 69%); ^{1}H-NMR (300 MHz, DMSO-d_6): δ 8.20 (d, *J*=8.7 Hz, 2H), 7.55 (d, *J*=8.7 Hz, 2H), 4.12–4.10 (m, 1H), 3.20 (dd, *J*=5.4, 4.5 Hz, 1H), 2.87 (dd, *J*=5.7, 2.7 Hz, 1H); LRMS (ESI) *m/z* 166 $[M+H]^+$; mp 78–80 °C.

2-(3,4-dimethoxyphenethylamino)-1-(4-nitrophenyl)ethanol (10)

To a solution of **9** (5 g, 0.03 mol) in dry THF (50 mL) stirred under N_2 at rt, was added 3,4-dimethoxyphenethylamine (5.6 mL, 0.033 mol), the reaction mixture was heated to reflux overnight. The solvent was evaporated under vacuum, and the residue was purified by chromatography (10:1 DCM-MeOH) to give the title compound as an a yellow solid (18 g, 56%); ^{1}H-NMR (300 MHz, $CDCl_3$): δ 8.16–8.14 (m, 2H), 7.60–7.57 (m, 2H), 6.82–6.68 (m, 3H), 5.58 (s, 1H), 4.77 (s, 1H), 3.70 (s, 3H), 3.68 (s, 3H), 2.74–2.60 (m, 6H), 1.51 (s, 1H); LRMS (ESI) *m/z* 347 $[M+H]^+$; mp 90–93 °C.

7,8-dimethoxy-1-(4-nitrophenyl)-2,3,4,5-tetrahydro-1H-benzo[d] azepine (11)

Compound **10** (10 g, 0.029 mmol) was treated with PPA (80 mL), the reaction was heated to 100 °C for 1.5 h. After cooling the reaction, the solution was poured into ice water, basidified by ammonia to adjust the pH>9, extracted with DCM (200 mL*2). The combined organic phase was washed with water and brine, dried over Na_2SO_4, filtered and concentrated to give the title compound as a red solid (11.3 g, 75%); ^{1}H-NMR (300 MHz, $CDCl_3$): δ 8.16–8.14 (m, 2H), 7.38–7.35 (m, 2H), 6.79 (s, 1H), 6.58 (s, 1H), 4.34–4.20 (m, 1H), 3.73 (s, 3H), 3.60 (s, 3H), 3.60–3.51 (m, 1H), 3.10–3.00 (m, 1H), 2.90–2.80 (m, 1H), 2.71–2.58 (m, 3H); LRMS (ESI) *m/z* 329 $[M+H]^+$; mp 131–134 °C.

4-(7,8-dimethoxy-2,3,4,5-tetrahydro-1H-benzo[d]azepin-1-yl)aniline (12)

Compound **11** (470 mg, 1.1 mmol) was added to a mixture of C_2H_5OH (30 mL) and H_2O (10 mL), followed by Fe (185 mg, 3.3 mmol) and several drops of HCl (aq). The reaction mixture was heated to reflux for 1 h. After cooling the reaction, saturated $NaHCO_3$ was added to adjust the pH>8, filtered through celite, washed with EtOAc, the combined filtrate was washed with brine, dried over Na_2SO_4, filtered and concentrated to give the title compound as a red solid (170 mg, 40%); ^{1}H-NMR (300 MHz, DMSO-d_6): δ 6.80–6.76 (m, 3H), 6.55–6.53 (m, 2H), 6.36 (s, 1H), 4.95 (brs, 2H), 4.19–4.16 (m, 1H), 3.71 (s, 3H), 3.50 (s, 3H), 3.20–3.17 (m, 1H), 3.05–2.84 (m, 3H), 2.83–2.76 (m, 2H), 2.48–2.40 (m, 1H); LRMS (ESI) *m/z* 229 $[M+H]^+$; mp 148–150 °C.

N-(4-(7,8-dimethoxy-3-(2-nitrophenylsulfonyl)-2,3,4,5-tetrahydro-1H-benzo[d]azepin-1-yl)phenyl)-2-nitrobenzenesulfonamide (13)

To a solution of **12** (4.5 g, 15.1 mmol), triethylamine (4.62 mL, 33.2 mmol) in dry DCM (150 mL) stirred under N_2 at 0 °C, was added 2-nitrobenzenesulfonyl chloride (7.03 g, 31.7 mmol) dropwise during 10 min, the reaction mixture was stirred at rt overnight. The mixture was washed with H_2O (20 mL) and brine (15 mL), dried over Na_2SO_4, filtered and concentrated. The crude product was then purified by chromatography (200:1 DCM-MeOH) to give the title compound as an amorphous yellow solid (4.5 g, 80%); ^{1}H-NMR (300 MHz, $CDCl_3$): δ 7.96–7.71 (m, 8H), 7.06–7.02 (m, 4H), 6.78 (s, 1H), 6.34 (s, 1H), 4.40–4.27 (m, 1H), 4.00–3.85(m, 1H), 3.70 (s, 3H), 3.68–3.61 (m, 1H), 3.47 (s, 3H), 3.40–3.31 (m, 2H), 2.81–2.96 (m, 2H); LRMS (ESI) *m/z* 669 $[M+H]^+$.

N-(4-(7,8-dimethoxy-3-(2-nitrophenylsulfonyl)-2,3,4,5-tetrahydro-1H-benzo[d]azepin-1-yl)phenyl)-2-nitro-N-(pent-4-ynyl)benzenesulfonamide (14)

To a solution of **13** (5 g, 7.48 mmol), triphenyl phosphine (4.56 g, 14.9 mmol) and hex-5-yn-1-ol (1.65 mL, 14.9 mmol) in dry DCM (30 mL) stirred under N_2 at 0 °C, was added DIAD (2.95 mL, 14.9 mmol) dropwise during 10 min, the reaction mixture was stirred at rt overnight. The mixture was washed with H_2O (20 mL) and brine (15 mL), dried over Na_2SO_4, filtered and concentrated. The crude product was then purified by chromatography (200:1 DCM-MeOH) to give the title compound as an white solid (4.5 g, 80%); ^{1}H-NMR (400 MHz, DMSO-d_6): δ 7.96–7.92 (m, 3H), 7.90–7.83 (m, 2H), 7.65–7.63 (m, 2H), 7.60–7.57 (m, 1H), 7.14 (s, 4H), 6.82 (s, 1H), 6.44 (s, 1H), 4.48–4.42 (m, 1H), 4.02–4.00 (m, 3H), 3.81–3.78 (m, 1H), 3.72 (s, 3H), 3.61–3.58 (m, 2H), 3.56 (s, 3H), 3.40–3.35 (m, 1H), 3.36–3.33 (m, 1H), 2.96–2.81 (m, 2H), 2.21–2.11 (m, 2H), 1.37 (s, 2H), 1.35 (s, 2H), 1.20–1.16 (m, 1H), 1.14–1.11 (m, 3H); LRMS (ESI) *m/z* 749 $[M+H]^+$.

Ethyl6-(N-(4-(7,8-dihydroxy-3-(2-nitrophenylsulfonyl)-2,3,4,5-tetrahydro-1H-benzo[d]azepin-1-yl)phenyl)-2-nitrophenylsulfonamido) hexanoate (15)

To a solution of **14** (160 mg, 0.20 mmol) in dry DCM (10 mL) stirred under N_2 at -78 °C, was added 1 mol/L BBr_3 (590 μL, 0.59 mmol) dropwise during 2 min. The reaction mixture was warmed to rt and stirred overnight. The reaction was quenched with MeOH (2 mL) when the solution was cooled to -78 °C. Then the solvent was removed under vacuo to give the title compound as brown solid without further purification; LRMS (ESI) *m/z* 783

$[M+H]^+$.

Ethyl6-(N-(4-(7,8-bis(methoxymethoxy)-3-(2-nitrophenylsulfonyl)-2,3,4,5-tetrahydro-1H-benzo[d]azepin-1-yl)phenyl)-2-nitrophenylsulfonamido) hexanoate (16)

To a solution of compound **15** (100 mg, 0.13 mmol) in dry DCM (10 mL) stirred at 0 °C, was added MOMBr (22 μL, 0.27 mmol), DIPEA (48 μL, 0.28 mmol), the reaction mixture was warmed to rt and stirred overnight. The solution was diluted with DCM (20 mL), washed with water and brine, dried over Na_2SO_4, filtered and concentrated. The residue was purified by chromatography with CH_2Cl_2 to afford the title compound as colorless oil without further purification; LRMS (ESI) *m/z* 888 $[M+NH_4]^+$.

6-(N-(4-(7,8-bis(methoxymethoxy)-3-(2-nitrophenylsulfonyl)-2,3,4,5-tetrahydro-1H-benzo[d]azepin-1-yl)phenyl)-2-nitrophenylsulfonamido) hexanoic acid (17)

To a solution of compound **16** (30 mg, 0.03 mmol) was dissolved in a mixture of THF/CH_3OH (1:1) (10 mL) stirred at rt, was added 2 mol/L NaOH (0.5 mL), the reaction mixture was stirred at rt for 1 h. The solvent was evaporated, 2 mol/L HCl was added to the residue to adjust pH<3, extracted with DCM (30 mL), washed with brine, dried over Na_2SO_4, filtered and concentrated. The residue was purified by chromatography (20: 1 DCM-MeOH) to afford the title compound as yellow oil (20 mg, 70%); ^{1}H-NMR (300 MHz, $CDCl_3$): δ 7.95–7.90 (m, 1H), 7.75–7.46 (m, 7H), 7.16–7.08 (m, 4H), 6.96 (s, 1H), 6.70 (s, 1H), 5.22 (s, 2H), 5.13–5.07 (m, 2H), 4.38–4.35 (m, 1H), 4.14–4.04 (m, 1H), 3.85–3.70 (m, 3H), 3.53 (s, 3H), 3.51–3.49 (m, 1H), 3.45 (s, 3H), 3.40–3.34 (m, 1H), 2.96–2.90 (m, 2H), 2.32 (t, *J*=7.2 Hz, 2H), 1.70–1.58 (m, 2H), 1.55–1.38 (m, 4H); LRMS (ESI) *m/z* 843 $[M+H]^+$.

6-(N-(4-(7,8-bis(methoxymethoxy)-3-(2-nitrophenylsulfonyl)-2,3,4,5-tetrahydro-1*H*-benzo[d]azepin-1-yl)phenyl)-2-nitrophenylsulfonamido)-N-(24-(8-(naphthalen-2-yl)-2,6-dioxo-1-propyl-1H-purin-3(2H,6H,7H)-yl)-21-oxo-4,7,10,13,16-pentaoxa-20-azatetracosyl) hexanamide (18a)

To a solution of compound **17** (110 mg, 0.13 mmol) and **7a** (91 mg, 0.13 mmol) in dry DMF (10 mL) stirred at rt, was added EDCI (31 mg, 0.16 mmol), HOBt (22 mg, 0.16 mmol) and DIPEA (68 μL, 0.38 mmol), the reaction mixture was stirred at rt overnight. The solvent was evaporated, and the residue was purified by chromatography (10:1 DCM-MeOH) to afford the title compound as an oil (80 mg, 40%); ^{1}H-NMR (400 MHz, DMSO-d_6): δ 8.66 (s, 1H), 8.22–8.21 (m, 1H), 7.96–7.81 (m, 4H), 7.60–7.51 (m, 11H), 7.10–7.06 (m, 2H), 7.05–7.02 (m, 2H), 6.65–6.58 (m, 2H), 5.14–5.10 (m, 2H), 5.02–5.01 (m, 2H), 4.28–4.27 (m, 3H), 4.16–4.15 (m, 1H), 3.98–3.94 (m, 1H), 3.72–3.65 (m, 12H), 3.62–3.55 (m, 14H), 3.45–3.41 (m, 3H), 3.32–3.25 (m, 5H), 3.15–3.07 (m, 6H), 2.22–2.12 (m, 2H), 2.02–1.93 (m, 5H), 1.77–1.65 (m, 9H), 0.95–0.93 (m, 3H); LRMS (ESI) *m/z* 1521 $[M+H]^+$.

6-(N-(4-(7,8-bis(methoxymethoxy)-3-(2-nitrophenylsulfonyl)-2,3,4,5-tetrahydro-1H-benzo[d]azepin-1-yl)phenyl)-2-nitrophenylsulfonamido)-N-(30-(8-(naphthalen-2-yl)-2,6-dioxo-1-propyl-1H-purin-3(2H,6H,7H)-yl)-27-oxo-4,7,10,13,16,19,22-heptaoxa-26-azatriacontyl)hexanamide (18b)

Compound **18b** (yield 38%) was prepared according to the methodology described for the preparation of compound **18a**. ^{1}H-NMR (400 MHz, DMSO-d_6): δ 8.85 (s, 1H), 8.36–8.34 (m, 1H), 7.93–7.87 (m, 4H), 7.67–7.51 (m, 11H), 7.25–7.06 (m, 4H), 7.74–6.63 (m, 2H), 5.19–5.10 (m, 4H), 4.38–4.24 (m, 3H), 3.75–3.72 (m, 1H), 3.68–3.62 (m, 10H), 3.61–3.52 (m, 12H), 3.36–3.34 (m, 15H), 3.27–3.21 (m, 5H), 3.19–3.11 (m, 5H), 2.28–2.19 (m, 4H), 2.07–1.99 (m, 5H), 1.75–1.65 (m, 9H), 1.55–1.53 (m, 3H); LRMS (ESI) *m/z* 1609 $[M+H]^+$.

6-(4-(7,8-bis(methoxymethoxy)-2,3,4,5-tetrahydro-1H-benzo[d]azepin-1-yl)phenylamino)-N-(24-(8-(naphthalen-2-yl)-2,6-dioxo-1-propyl-1H-purin-3(2H,6H,7H)-yl)-21-oxo-4,7,10,13,16-pentaoxa-20-azatetracosyl)hexanamide (19a)

To a solution of compound **18a** (45 mg, 0.03 mmol) and K_2CO_3 (40 mg, 0.3 mmol) in dry DMF (10 mL) stirred at rt, was added PhSH (30 μL, 0.3 mmol), the reaction mixture was stirred at rt overnight. The solvent was evaporated under vacuo, the residue was purified by silica gel thin-layer chromatography (9:1 DCM-MeOH) to afford the title compound as a yellow solid (20 mg, 60%); ^{1}H-NMR (400 MHz, DMSO-d_6): δ 8.79 (s, 1H), 8.32 (d, *J*=8.8 Hz, 1H), 8.02–8.00 (m, 1H), 7.92–7.90 (m, 1H), 7.88–7.83 (m, 1H), 7.70–7.69 (m, 1H), 7.52–7.50 (m, 2H), 7.21–7.19 (m, 1H), 6.99 (s, 1H), 6.83–6.81 (m, 2H), 6.74 (d, *J*=7.6 Hz, 2H), 6.29 (d, *J*=8 Hz, 2H), 5.24–5.23 (m, 2H), 5.12–5.11 (m, 2H), 4.28–4.24 (m, 3H), 3.94–3.89 (m, 1H), 3.79–3.75 (m, 1H), 3.61–3.60 (m, 12H), 3.56–3.52 (m, 14H), 3.44 (s, 3H), 3.35–3.32 (m, 5H), 3.14–3.08 (m, 2H), 2.89–2.86 (m, 4H), 2.32–2.30 (m, 2H), 2.20–2.16 (m, 5H), 1.88–1.73 (m, 5H), 1.54–1.51 (m, 4H), 0.88–0.84 (m, 3H); LRMS (ESI) *m/z* 1151 $[M+H]^+$.

6-(4-(7,8-bis(methoxymethoxy)-2,3,4,5-tetrahydro-1H-benzo[d]azepin-1-yl)phenylamino)-N-(30-(8-(naphthalen-2-yl)-2,6-dioxo-1-propyl-1H-purin-3(2H,6H,7H)-yl)-27-oxo-4,7,10,13,16,19,22-heptaoxa-26-azatriacontyl)hexanamide (19b)

Compound **19b** (yield 55%) was prepared according to the methodology described for the preparation of compound **19a**; ^{1}H-NMR (400 MHz, DMSO-d_6): δ 8.85 (s, 1H), 8.36–8.34 (m, 1H), 8.06–8.03 (m, 1H), 7.95–7.92 (m, 1H), 7.87–7.85 (m, 1H), 7.55–7.52 (m, 2H), 7.22–7.21 (m, 1H), 7.00–6.99 (m, 1H), 6.80–6.77 (m, 4H), 6.39–6.36 (m, 2H), 5.25–5.24 (m, 2H), 5.11–5.09 (m, 2H), 4.32–4.30 (m, 1H), 4.28 (t, *J*=16Hz, 2H), 3.85–3.77 (m, 2H), 3.63–3.62 (m, 1H), 3.61–3.52 (m, 32H), 3.45 (s, 3H), 3.41–3.31 (m, 5H), 3.08–3.05 (m, 2H), 2.95–2.90 (m, 3H), 2.20–2.18 (m, 5H), 1.78–1.72 (m, 5H), 1.69–1.52 (m, 8H), 0.88–0.86 (m, 3H); LRMS (ESI) *m/z* 1239 $[M+H]^+$.

6-(4-(7,8-dihydroxy-2,3,4,5-tetrahydro-1H-benzo[d]azepin-1-yl) phenylamino)-N-(24-(8-(naphthalen-2-yl)-2,6-dioxo-1-propyl-1H-purin-3(2H,6H,7H)-yl)-21-oxo-4,7,10,13,16-pentaoxa-20-azatetracosyl) hexanamide (20a)

To a solution of compound **19a** (12 mg, 0.01 mmol) in DCM (4 mL) stirred at rt, was added TFA (1 mL), the reaction mixture was stirred at rt for 30 min. The solvent was evaporated under vacuo, the residue was purified by silica gel thin-layer chromatography (9:1 DCM-MeOH) to afford the title compound as an amorphous white solid (6.5 mg, 60%). ^{1}H-NMR (400 MHz, DMSO-d_6): δ 8.81 (brs, 1H), 8.71 (s, 1H), 8.66 (brs, 1H), 8.26–8.23 (m, 1H), 8.04–7.93

(m, 3H), 7.96–7.80 (m, 2H), 7.59–7.56 (m, 2H), 6.84 (d, *J*=10.4 Hz, 2H), 6.61–6.54 (m, 3H), 6.05 (s, 1H), 5.61–5.54 (m, 1H), 4.33–4.31 (m, 1H), 4.10 (t, *J*=9.6 Hz, 2H), 3.87 (t, *J*=8.8 Hz, 2H), 3.46–3.41 (m, 12H), 3.35–3.33 (m, 16H), 3.07–3.01 (m, 4H), 2.96–2.91 (m, 2H), 2.18–2.13 (m, 2H), 2.06–1.95 (m, 5H), 1.60–1.48 (m, 9H), 0.87 (t, *J*=8 Hz, 3H); ^{13}C-NMR (100 MHz, DMSO-d_6) δ 179.67, 172.45, 171.76, 154.73, 151.15, 150.52, 148.31, 143.64, 143.62, 134.24, 133.88, 133.11, 130.21, 130.10, 129.65, 129.09, 128.97, 128.24, 128.12, 127.72, 127.43, 127.03, 126.42, 124.11, 118.07, 117.12, 112.53, 70.19, 70.15, 69.97, 69.93, 68.55, 68.52, 51.01, 45.95, 44.81, 43.28, 43.18, 42.63, 36.26, 36.15, 35.88, 33.15, 29.85, 29.77, 29.02, 26.90, 25.66, 24.39, 21.35, 14.8, 11.70; LRMS (ESI) *m/z* 1063 $[M+H]^+$.

6-(4-(7,8-dihydroxy-2,3,4,5-tetrahydro-1H-benzo[d]azepin-1-yl) phenylamino)-N-(30-(8-(naphthalen-2-yl)-2,6-dioxo-1-propyl-1H-purin-3(2H,6H,7H)-yl)-27-oxo-4,7,10,13,16,19,22-heptaoxa-26-azatriacontyl)hexanamide (20b)

Compound **20b** was prepared according to the methodology described for the preparation of compound **20a**. Yield: 55%. ^{1}H-NMR (400 MHz, DMSO-d_6): δ 8.78 (brs, 1H), 8.71 (s, 1H), 8.67 (brs, 1H), 8.26–8.23 (m, 1H), 8.04–7.93 (m, 3H), 7.96–7.80 (m, 2H), 7.60–7.58 (m, 2H), 6.85 (d, *J*=8.4 Hz, 2H), 6.59–6.55 (m, 3H), 6.06 (s, 1H), 5.56–5.54 (m, 1H), 5.32–5.39 (m, 1H), 4.33–4.31 (m, 1H), 4.11 (t, *J*=9.6 Hz, 2H), 3.88 (t, *J*=8.8 Hz, 2H), 3.45–3.38 (m, 30H), 3.06–3.04 (m, 5H), 2.98–2.95 (m, 2H), 2.85–2.65 (m, 3H), 2.15–2.12 (m, 2H), 2.15–1.96 (m, 8H), 2.08–1.96 (m, 8H), 1.60–1.49 (m, 9H), 0.86 (t, *J*=8 Hz, 3H); ^{13}C-NMR (100 MHz, *d*-DMSO) δ 174.77, 172.42, 171.73, 151.14, 148.33, 143.67, 133.92, 133.09, 130.11, 129.56, 129.08, 128.98, 128.25, 127.79, 127.47, 126.49, 124.07, 118.03, 112.53, 70.20, 69.98, 69.93, 68.55, 68.52, 50.88, 45.92, 44.77, 43.27, 43.17, 42.66, 36.27, 36.16, 35.89, 33.14, 29.86, 29.77, 29.02, 26.90, 25.65, 24.38, 22.55, 21.34, 14.42, 11.69; LRMS (ESI) *m/z* 1151 $[M+H]^+$.

N-(24-(8-(naphthalen-2-yl)-2,6-dioxo-1-propyl-1H-purin-3(2H,6H,7H)-yl)-21-oxo-4,7,10,13,16-pentaoxa-20-azatetracosyl)hexanamide (21a)

To a solution of compound **7a** (28 mg, 0.04 mmol) and hexanoic acid (5.88 μL, 0.044 mmol) in dry DMF (2 mL) stirred at rt, was added EDCI (9.2 mg, 0.048 mmol), HOBt (6.5 mg, 0.048 mmol) and DIPEA (14 μL, 0.08 mmol), the reaction mixture was stirred at rt overnight. The solvent was evaporated under vacuo, the residue was purified by chromatography with CH_2Cl_2/CH_3OH (9:1) to afford the title compound as an amorphous white solid (21 mg, 70 %); ^{1}H-NMR (400 MHz, DMSO-d_6): δ 14.01 (s, 1H), 8.72 (s, 1H), 8.23–8.22 (m, 1H), 8.05–7.98 (m, 3H), 7.83–7.76 (m, 2H), 7.60–7.57 (m, 2H), 4.10 (t, *J*=8.4 Hz, 2H), 3.87 (t, *J*=8.8 Hz, 2H), 3.46–3.42 (m, 16H), 3.38–3.36 (m, 8H), 3.07–3.00 (m, 4H), 2.13 (t, *J*=9.6 Hz, 2H), 2.03–1.98 (m, 4H), 1.63–1.55 (m, 6H), 1.49–1.41 (m, 2H), 0.86 (t, *J*=8 Hz, 3H), 0.83–0.85 (m, 3H); LRMS (ESI) *m/z* 697 $[M+H]^+$.

N-(30-(8-(naphthalen-2-yl)-2,6-dioxo-1-propyl-1H-purin-3(2H,6H,7H)-yl)-27-oxo-4,7,10,13,16,19,22-heptaoxa-26-azatriacontyl) hexanamide (21b)

Compound **21b** was prepared according to the methodology described for the preparation of compound **21a**. Yield: 71%; ^{1}H-NMR (400 MHz, DMSO-d_6): δ 14.01 (s, 1H), 8.71 (s, 1H), 8.25–8.22 (m, 1H), 8.05–7.96 (m, 3H), 7.83–7.76 (m, 2H), 7.60–7.57 (m, 2H), 4.11 (t, *J*=8.4 Hz, 2H), 3.87 (t, *J*=8.8 Hz, 2H), 3.46–3.42 (m, 24H), 3.40–3.35 (m, 8H), 3.07–3.01 (m, 4H), 2.15 (t, *J*=9.6 Hz, 2H), 2.03–1.98 (m, 4H), 1.60–1.54 (m, 6H), 1.46–1.45 (m, 2H), 0.86 (t, *J*=8 Hz, 3H), 0.83–0.84 (m, 3H); LRMS (ESI) *m/z* 883 $[M+H]^+$.

Acknowledgements

This study was supported by the '100 Talents Project' of CAS to Ye-chun XU and National S&T Major Project (No 2012ZX09301-001-005).

Author contribution

Jing-kang SHEN, Lin-yin FENG, and Ye-chun XU designed the research; Jian SHEN, Tao MENG, Lei ZHANG, and Wan-ling SONG performed the research; Xin WANG and Lin CHEN contributed analytical tools and reagents; Jian SHEN and Tao MENG analyzed data; and Jian SHEN wrote the paper.

References

1 Milligan G. G protein-coupled receptor dimerization: function and ligand pharmacology. Mol Pharmacol 2004; 66: 1–7.
2 Carriba P, Navarro G, Ciruela F, Ferre S, Casado V, Agnati L, *et al*. Detection of heteromerization of more than two proteins by sequential BRET-FRET. Nat Methods 2008; 5: 727–33.
3 George SR, O'Dowd BF, Lee SP. G-protein-coupled receptor oligomerization and its potential for drug discovery. Nat Rev Drug Discov 2002; 1: 808–20.
4 Milligan G. G-protein-coupled receptor heterodimers: pharmacology, function and relevance to drug discovery. Drug Discov Today 2006; 11: 541–9.
5 Franco R. Dopamine D_1 and adenosine A_1 receptors form functionally interacting heteromeric complexes. PNAS 2000; 97: 8606–11.
6 Franco R, Lluis C, Canela EI, Mallol J, Agnati L, Casadó V, *et al*. Receptor-receptor interactions involving adenosine A1 or dopamine D1 receptors and accessory proteins. J Neural Transm 2007; 114: 93–104.
7 Popoli P, Gimenez-Llort L, Pezzola A, Reggio R, Martinez E, Fuxe K. Adenosine A_1 receptor blockade selectively potentiates the motor effects induced by dopamine D_1 receptor stimulation in rodents. Neurosci Lett 1996; 218: 209–13.
8 Liu Z, Zhang J, Zhang A. Design of multivalent ligand targeting G-protein-coupled receptors. Curr Pharm Des 2009; 15: 682–718.
9 Russo O, Berthouze M, Giner M, Soulier JL, Rivail L, Sicsic S, *et al*. Synthesis of specific bivalent probes that functionally interact with 5-HT(4) receptor dimers. J Med Chem 2007; 50: 4482–92.
10 Christopoulos A, Grant MK, Ayoubzadeh N, Kim ON, Sauerberg P, Jeppesen L, *et al*. Synthesis and pharmacological evaluation of dimeric muscarinic acetylcholine receptor agonists. J Pharmacol Exp Ther 2001; 298: 1260–8.
11 Peng X, Neumeyer JL. Kappa receptor bivalent ligands. Curr Top Med Chem 2007; 7: 363–73.
12 Soriano A, Ventura R, Molero A, Hoen A, Casado V, Cortes A, *et al*. Adenosine A2A receptor-antagonist/dopamine D2 receptor-agonist bivalent ligands as pharmacological tools to detect A2A-D2 receptor heteromers. J Med Chem 2009; 52: 5590–602.
13 Miiller C, Schobert U, Hipp J, Geis U, Frobenius W, Pawlowski M. Configurationally stable analogs of styrylxanthines as A_{2A} adenosine receptor antagonists. Eur J Med Chem 1997; 32: 709–19.
14 González MP, Terán C, Teijeira M. Search for new antagonist ligands

for adenosine receptors from QSAR point of view. How close are we? Med Res Rev 2008; 28: 329–71.
15 Neumeyerc JL, Kula NS, Bergman J, Baldessarini RJ. Receptor affinities of dopamine D_1 receptor-selective novel phenylbenzazepines. Eur J Pharmacol 2003; 474: 137–40
16 Zhang J, Xiong B, Zhen XC, Zhang A. Dopamine D_1 receptor ligands: Where are we now and where are we going? Med Res Rev 2009; 29: 272–94.
17 Jiarpinitnun C, Kiessling L. Unexpected enhancement in biological activity of a GPCR ligand induced by an oligoethylene glycol substituent. J Am Chem Soc 2010; 132: 8844–5.
18 Mammen M, Shakhnovich E, Whitesides G. Using a convenient, quantitative model for torsional entropy to establish qualitative trends for molecular processes that restrict conformational freedom. J Org Chem 1998; 63: 3168–75.
19 Huber D, Lober S, Hubner H, Gmeiner P. Bivalent molecular probes for dopamine D_2-like receptors. Bioorg Med Chem 2012; 20: 455–66.
20 Bakthavachalam V, Baindur N, Madras BK, Neumeyer JL. Fluorescent probes for dopamine receptors: synthesis and characterization of fluorescein and 7-nitrobenz-2-oxa-l,3-diazol-4-y conjugates of D-1 and D-2 receptor ligands. J Med Chem 1991; 34: 3235–41.
21 Wu P, Brand L. Resonance energy transfer: methods and applications. Anal Biochem 1994; 218: 1–13.
22 Jaakola VP, Griffith MT, Hanson MA, Cherezov V, Chien EY, Lane JR, *et al*. The 2.6 angstrom crystal structure of a human A_{2A} adenosine receptor bound to an antagonist. Science 2008; 322: 1211–7.
23 Okada T, Sugihara M, Bondar AN, Elstner M, Entel P, Buss V. The retinal conformation and its environment in rhodopsin in light of a new 2.2 A crystal structure. J Mol Biol 2004; 342: 571–83.
24 Cherezov V, Rosenbaum DM, Hanson MA, Rasmussen SG, Thian FS, Kobilka TS, *et al*. High-resolution crystal structure of an engineered human beta(2)-adrenergic G protein-coupled receptor. Science 2007; 318: 1258–65.
25 Shimamura T, Shiroishi M, Weyand S, Tsujimoto H, Winter G, Katritch V, *et al*. Structure of the human histamine H_1 receptor complex with doxepin. Nature 2011; 475: 65–70.
26 Hanson MA, Roth CB, Jo E, Griffith MT, Scott FL, Reinhart G, *et al*. Crystal structure of a lipid G protein-coupled receptor. Science 2012; 335: 851–5.
27 Chien EY, Liu W, Zhao Q, Katritch V, Han GW, Hanson MA, *et al*. Structure of the human dopamine D_3 receptor in complex with a D_2/D_3 selective antagonist. Science 2010; 330: 1091–5.
28 Tarakanov AO, Fuxe KG. Triplet puzzle: homologies of receptor heteromers. J Mol Neurosci 2010; 41: 294–303.
29 Tarakanov AO, Fuxe KG. The triplet puzzle of homologies in receptor heteromers exists also in other types of protein-protein interactions. J Mol Neurosci 2011; 44: 173–7.
30 Kuhhorn J, Hubner H, Gmeiner P. Bivalent dopamine D_2 receptor ligands: synthesis and binding properties. J Med Chem 2011; 54: 4896–903.